Published in final edited form as:
J Control Release. 2008 September 10; 130(2): 107–114. doi:10.1016/j.jconrel.2008.05.024.

Receptor targeted polymers, dendrimers, liposomes: Which nanocarrier is the most efficient for tumor-specific treatment and imaging?

Maha Saad, **Olga B. Garbuzenko**, **Elizabeth Ber**, **Pooja Chandna**, **Jayant J. Khandare**, **Vitaly P. Pozharov**, and **Tamara Minko***
Department of Pharmaceutics, Ernest Mario School of Pharmacy, Rutgers, The State University of New Jersey, Piscataway, NJ 08854, USA

Abstract

To compare the influence of different characteristics of nanocarriers on the efficacy of chemotherapy and imaging, we designed, characterized, and evaluated three widely used nanocarriers: linear polymer, dendrimer and liposome *in vitro* and *in vivo*. These nanocarriers delivered the same anticancer drug (paclitaxel) and/or imaging agent (Cy5.5). A synthetic analog of LHRH peptide targeted to receptors overexpressed on the membrane of cancer cells was attached to the nanocarriers as a tumor targeting moiety. Significant differences were found between various studied non-targeted carriers in their cellular internalization, cytotoxicity, tumor and organ distribution and anticancer efficacy. LHRH peptide substantially enhanced intratumoral accumulation and anticancer efficacy of all delivery systems and minimized their adverse side effects. For the first time, the present study revealed that the targeting of nanocarriers to tumor-specific receptors minimizes the influence of the architecture, composition, size and molecular mass of nanocarriers on the efficacy of imaging and cancer treatment.

Keywords

Nanocarriers; LHRH peptide; Tumor-specific targeting; Adverse side effects; Imaging

1. Introduction

Nanotechnology products are most often used as pharmaceutical nanocarriers for delivering drugs or imaging agents to the site of the action in desired quantities and for releasing therapeutic loads with a specific time profile. Linear and branched polymers, dendrimers, quantum dots, nanoparticles, nanospheres, nanotubes, nanocrystals, nanogels, liposomes, micelles, as well as other types of nanocarriers are being employed in different fields of medicine for diagnostics, imaging, treatment and prophylactics of many pathological conditions, including cancer [1–21]. In contrast to earlier developed nanotherapeutics, which had a relatively simple two-component drug-carrier composition, modern nanocarriers often include other active ingredients that perform different functions for enhancing cellular uptake and efficiency of the main drug. Therefore, they limit adverse side effects, provide drug release with a predetermined profile in the certain compartment of an organ, tissue or cell, and prevent the development and/or suppression of the existent drug resistance, etc.

*Corresponding author. Department of Pharmaceutics, Ernest Mario School of Pharmacy, Rutgers, The State University of New Jersey, 160 Frelinghuysen Road, Piscataway, NJ 08854-8020, USA. Tel.: +1 732 445 3831x214; fax: +1 732 445 3134. minko@rci.rutgers.edu (T. Minko)..

The increase in complexity and performed functions of nanocarriers actually converts them into multifunctional nanotherapeutical products [22].

While nanocarriers are currently being extensively used for delivering imaging and cytotoxic agents to tumors, there are no studies which compare different types of carriers containing the same active ingredients in similar experimental conditions in both *in vitro* and *in vivo* settings. The present study fills this gap and is aimed at investigating the three most widely used types of nanocarriers with different architecture, size, and molecular mass (linear polymer, branched star-like dendrimer and liposomes) containing a near-infrared cyanine Cy5.5 dye (imaging agent) and/or paclitaxel (anticancer drug with low aqueous solubility). In addition, a synthetic analog of luteinizing hormone-releasing hormone (LHRH peptide) was attached to the nanocarriers and is used as a targeting moiety (ligand to LHRH receptors that are overexpressed in the plasma membrane of several types of cancer cells and are not expressed detectably in normal visceral organs) [23,24]. Analysis of experimental *in vitro* and *in vivo* data at the first time revealed a very important phenomenon that can potentially have a significant impact on drug delivery in general and cancer chemotherapy in particular. We found that targeting drug carriers to extracellular receptors overexpressed in the plasma membrane of cancer cells, eliminated the differences between the carriers in terms of their internalization by cancer cells, cytotoxicity, tumor and organ distribution, adverse side effects and antitumor activity. Specific targeting of nanocarriers to cancer cells substantially enhanced cytotoxicity and antitumor efficacy of all delivery systems to the comparable and exceptionally high level and limited their adverse side effects despite of the considerable differences in the size, molecular mass of the components, composition and architecture of the carriers. The present study sends an important message that the architecture, composition, size and molecular mass of the receptor-targeted drug nanocarriers can be selected based on other than anticancer efficacy considerations (cost, type of active ingredients, difficulties in production, stability, patient compliance, etc.) ensuring that the high efficacy and low adverse side effects could be achieved automatically by tumor targeting.

2. Methods and materials

2.1. Nanocarriers

Three types of delivery systems (DS) were designed and prepared based on different nanocarriers: linear polymer, branched star-like dendrimer and liposomes (Fig. 1a). All systems contained at least one of the following components: (1) a synthetic analog of luteinizing hormone-releasing hormone (LHRH) decapeptide as a targeting moiety; (2) near-infrared cyanine Cy5.5 fluorescent dye as an imaging agent and (3) paclitaxel (TAX) as an anticancer drug. LHRH peptide provided targeting of an entire DS to the receptors overexpressed in many types of cancer cells. TAX was selected as an example of a highly effective chemotherapeutic agent with low aqueous solubility. Cy5.5 represents a class of very effective dyes currently used as cancer imaging agents. The systems were prepared and characterized using procedures previously developed in our laboratory [7,23–28]. Based on the results of dynamic light scattering and atomic force microscope measurements, the average size of dendrimers, PEG polymers, and liposomes were about 5, 30 and 100 nm respectively. The preparation of each DS is briefly summarized below.

2.1.1. Linear PEG polymers—Cy5.5–PEG conjugate was prepared by the coupling of Cy5.5 NHS ester activated by triethanolamine with Bis-diamine PEG. The resulting compound with one free amine group at the terminal was coupled with succinic acid to form Cy-5.5–PEG–COOH complex, which further reacted with LHRH–NH_2 to form an amide conjugate. To synthesize PEG–TAX conjugate, α,ω bis PEG–citric acid containing carboxyl

end groups at the terminals was coupled with hydroxyl groups in paclitaxel to form an ester conjugate. On each stage of the synthesis, the resulting solution was filtered and the filtrate was dialyzed extensively with dimethyl sulfoxide (DMSO) using a dialysis membrane (molecular mass cut off=2000 Da) for 24 h to remove unreacted low molecular mass components. Furthermore, the conjugate was purified using a size exclusion Sephadex G10 column and dried under the vacuum at room temperature.

2.1.2. Dendrimers—Polyamidoamine (PAMAM) generation four hydroxyl dendrimer conjugate with hydroxyl functional group was conjugated with carboxylic group of boc glycine·HCl and further conjugated with Cy5.5 to form dendrimer–glycine–Cy5.5 conjugate. The latter was conjugated with succinic acid to form a dendrimer–glycine–Cy5.5–carboxylic acid conjugate, which in turn was coupled with LHRH. TAX was attached to succinic acid, which is reacted on an equimolar basis with hydroxyl group in paclitaxel to form a paclitaxel–succinic acid conjugate leaving one free carboxyl group for further conjugation with hydroxyl terminal of the dendrimer. The solution of each dendrimeric complex was filtered and the filtrate was dialyzed extensively with anhydrous DMSO for 24 h to remove unreacted components. The dendrimer was further purified using a size exclusion Sephadex G10 column.

2.1.3. Liposomes—DSPE-PEG (1,2-distearoyl-sn-glycero-3-phosphoetanol amine-*N*-aminopolyethylene glycol-M_w ~2000 ammonium salt-polyethylene glycol) was conjugated with LHRH and Cy5.5 as described above. Egg phosphotidyl choline, cholesterol, DSPE-PEG, DSPE-PEG–Cy5.5 and/or DSPE-PEG–LHRH conjugates were dissolved in chloroform, evaporated to a thin film in rotary evaporator, rehydrated with 0.9% NaCl and gradually extruded through 200 nm and 100 nm pore size polycarbonate filters with an extruder apparatus. The final phospholipid concentration was 20 mM. Paclitaxel was diluted in methanol (50 mg/ml) and added to the liposome suspension in a ratio of 10%/ 90% v/v [25]. The non-encapsulated drug was separated from liposomes by extensive dialyses against saline. The amount of TAX incorporated into liposomes was determined by high-performance liquid chromatography (HPLC). The encapsulation efficacy of TAX ranged from 55 to 60% in different series of experiments. For the determination of the stability of liposomal TAX formulations, drug release from liposomes suspended in a micro-dialysis system was monitored by periodic withdrawals of drug released into the neutral buffer, and detected by HPLC. At 4 °C, leakage from both targeted and non-targeted liposomes was minimal, with less than 5% of TAX lost after 1 month, which is convenient for storage of vesicles.

The concentration of TAX in DS was determined by high-performance liquid chromatography (HPLC) using symmetry C18 column (150 mm×4.6 mm, Water Corporation) operated at room temperature. The mobile phase consisted of 20 mM ammonium acetate (pH 5)/acetonitrile/methanol 50:40:10 v/v/v; the flow rate was set to 1.0 ml/min, wavelength 227 nm. The chromatographic apparatus consisted of a Model 1525 pump (Waters Instruments, Milford, MA, USA), a Model 717 Plus auto-injector (Waters Instruments) and a Model 2487 variable wavelength UV detector (Waters Instruments) connected to the Millennium software.

2.2. In vitro experiments

The experiments were carried out on human small H69 and A549 non-small lung cancer cells. The expression of a targeted LHRH receptor was measured in mRNA isolated from cell lysates and commercially available mRNA from healthy human organs by the reverse transcription polymerase chain reaction (RT-PCR) as previously described [23,26,29]. In part of the experiments, LHRH peptide was labeled with rhodamine as previously described

[24] and incubated within 48 h with lung cancer cells. Cells were fixed, washed, and labeled LHRH was visualized by a fluorescent microscope. In this series of experiments, cellular nuclei were labeled with Hoechst 33258 fluorescent dye. Cellular internalization, accumulation, and distribution of different conjugates labeled with Cy5.5 were analyzed by a confocal microscope. To assess intracellular distribution of the substances, ten optical sections, known as a *z*-series, were scanned sequentially along the vertical (*z*) axis from the top to the bottom of the cell. The intensity of fluorescence in each scan was compared with that in the first (top of the cell) image. Average intensity through all 10 images was used to characterize the penetration and accumulation of the analyzed substance in the cell. Cellular viability was analyzed by the modified MTT assay as previously described [30,31] after 48 h incubation with different DS and appropriate controls. Based on the results of the test, the IC_{50} doses (the concentrations which kill 50% of cells) were calculated for free paclitaxel and TAX-containing DS.

2.3. In vivo experiments

Experiments were carried out on nude mice bearing subcutaneous rapidly grown xenografts of human lung cancer cells as previously described [32,33]. Each experimental group consisted of 8–10 animals. According to the approved institutional animal use protocol, the tumor was measured by a caliper every day and its volume was calculated as $d^2 \times D/2$ where d and D are the shortest and longest diameter of the tumor in mm, respectively. When the tumor reached a mean size of 500 mm^3, mice were treated intravenously (via the tail vein) with different DS and appropriate control substances. The paclitaxel concentration was equal to 2.5 mg/kg for free TAX and all TAX-containing DS. At the end of the experiments, apoptosis induction in the tumor and other organs was assessed by measuring the enrichment of histone-associated DNA fragments (mono- and oligonucleosomes) in tissue homogenates as previously described [23]. No group of mice showed any significant differences in mass change. In a separate series of the experiments, different labeled DS were injected intravenously to untreated mice with tumor size about 1500 mm^3 and their distribution in the entire body of mice, excised tumor and other organs were analyzed in anesthetized animals by *in vivo* imaging using IVIS Xenogen imaging system.

2.4. Statistics

The results are expressed as mean± SD from 4–8 independent measurements. Statistical analysis was performed as a one-way analysis of variance (ANOVA) and comparisons among groups were performed by independent sample *t*-tests.

3. Results

3.1. Different nanocarriers

Three different types of widely used nanocarriers and delivery systems (DS) were prepared and characterized in the present study (Fig. 1a). The first DS consisted of a linear poly(ethylene glycol) (PEG) polymer as a carrier, LHRH peptide as a targeting moiety and paclitaxel (TAX) as an anticancer drug or near-infrared cyanine dye Cy5.5 as an imaging agent. The second and third systems employed a branched PAMAM polymer or PEGylated liposome respectively as carriers in combination with LHRH peptide, Cy5.5, and/or TAX. In all systems, LHRH peptide and Cy5.5 dye were conjugated to PEG or PAMAM polymer via a non-biodegradable amide bond, while TAX was conjugated to a polymer via biodegradable ester bond or was incorporated in the phospholipid bilayer of liposomal membrane (Fig. 1a). Drug concentration in different DS was measured by HPLC. Structure, size, and molecular mass of the designed DS were confirmed by atomic force microscope, MALDI-TOFF mass spectrometry, ^1H NMR spectroscopy, dynamic light scattering and molecular modeling. The prepared three types of nanocarrier-based DS covered a wide

range of characteristics of nanocarriers including size (5–200 nm), molecular mass of polymers (from ~3 kDa of linear PEG to ~15 kDa of dendrimer) and architecture (linear, branched and vesicular).

3.2. LHRH receptors are overexpressed in the plasma membrane of cancer cells and are not expressed detectably in normal visceral organs

Two series of experiments were performed to show the localization and expression of targeted LHRH receptors in cancer cells. In the first series, drug sensitive and multidrug resistant human lung cancer cells were incubated with LHRH peptide labeled by rhodamine (red fluorescence). Cellular nuclei were labeled with nuclear dye Hoechst 33258 (blue fluorescence). Fluorescence was analyzed by a fluorescent microscope and photographed. Light and both fluorescence filters (red and blue) images were digitally combined. Typical representative images of A549 human lung cancer cells are shown in Fig. 1b. It is clear from the images, that LHRH peptide (ligand) bound to the corresponding LHRH receptors is localized predominately in the plasma membrane of cancer cells. The measurement by RT-PCR of the expression of genes encoding LHRH receptors in different human lung cancer cells and in various healthy human organs (liver, kidney, spleen, heart, lung) showed that LHRH receptors are overexpressed in human lung cancer cells and not detectably expressed in healthy lungs and other visceral organs (Fig. 1c). These data confirmed our previous findings in ovarian, breast, and prostate cancer cells as well as cancerous and healthy reproductive organs [23,29] and provides the rationale of using LHRH peptide as a targeting moiety/penetration enhancer to target different DS specifically to tumors and facilitate their uptake by cancer cells.

3.3. Receptor-based targeting to cancer cells improves penetration, accumulation and intracellular distribution of delivery nanocarriers

Cellular uptake and intracellular distribution of fluorescent dye and different nanocarriers labeled with Cy5.5 were studied by confocal fluorescence microscopy using viable A549 human lung cancer cells. The concentration of fluorescent dye in the incubation media was the same (50 nM) for free dye and dye delivered by various carriers. It was found that incubation of cancer cells with free Cy5.5 led to the accumulation of only a trace amount of the applied dye in cancer cells (Fig. 2a, panel 1; Fig. 2b, bar 1). Moreover, the distribution of the dye throughout the body of the cells was highly inhomogeneous with almost a 5-fold difference in the dye concentration from the top to the bottom of the cells (curve 1 in Fig. 2c). This distribution reflects the poor penetration ability of free Cy5.5 from the medium contacted with the top of the cell to the bottom of the cell attached to a base of the incubation dish. In contrast to the free dye, labeled non-targeted carriers (DS without LHRH peptide) showed significantly higher penetration ability and accumulation in cancer cells (Fig. 2a, panel 2; Fig. 2b, bar 2). However, different carriers demonstrated substantial variations in their accumulation in cancer cells (Fig. 2b). While the labeled linear PEG polymer showed the lowest accumulation, liposomes demonstrated the highest penetration ability and accumulation inside cancer cells (compare bars 2, 4 and 6 in Fig. 2b). The concentration difference between the top and bottom of the cancer cells was about 40% for all non-targeted carriers. Targeting to cancer cells by LHRH peptide significantly improved penetration and accumulation of all carriers and decreased variations in their concentrations through the cell (compare bars and curves 3, 5, and 7 in Fig. 2b and c). It should also be stressed that targeting substantially decreased the differences in the accumulation between different carriers. While the difference in the total accumulation inside cancer cells between different carriers reached 3-folds for non-targeted carriers, cancer targeting by LHRH peptide decreased this difference to only 10–20%.

3.4. LHRH peptide enhances cytotoxicity of anticancer drug

Cytotoxicity of free TAX and different DS containing paclitaxel was measured by the MTT assay with appropriate controls. It was found that all non-targeted and cancer-targeted DS by themselves (without an anticancer drug) were not toxic (Fig. 3a). The toxicity of different non-targeted carriers containing TAX varied more than 100 times. While linear PEG polymer–TAX conjugate had the lowest cytotoxicity, PAMAM–TAX dendrimer showed the highest toxicity (Fig. 3b). The incorporation of LHRH peptide as a cancer targeting moiety dramatically (5–800 times) enhanced toxicity of all DS and substantially eliminated differences in IC_{50} doses between the different targeted DS (compare bars 11, 13 and 15 in Fig. 3b).

3.5. Receptor targeting leads to the preferential accumulation of nanocarriers in the tumor and limits adverse side effects on healthy organs

Body distribution of different non-targeted and tumor-targeted nanocarriers was studied by *in vivo* imaging after systemic administration of the nanocarriers labeled with Cy5.5 to mice bearing xenografts of A549 human lung cancer cells. Animals were anesthetized with Isoflurane and photographed in visible and fluorescent light using IVIS imaging systems 48 h after the injection. The intensity of the fluorescence was represented on composite light/fluorescent images by different colors with blue color reflecting the lowest fluorescence intensity and red color — the highest intensity. After photographing, animals were euthanized, tumor and organs were excised, photographed, and processed similarly to the images of an entire animal. Typical representative images and histograms of fluorescence distribution in mice obtained in this series of the experiments are presented in Fig. 4. The data showed that a substantial fraction of all injected non-targeted nanocarriers was accumulated in the tumor. However, significant amounts of non-targeted nanocarriers were found in healthy organs. In addition to the tumor, substantial amounts of linear PEG were found in the liver and kidney, while liposomes and PAMAM dendrimers accumulated in significant quantities in the liver, spleen, and kidney respectively. Tumor targeting by LHRH peptide significantly changed body distribution of all tumor-targeted nanocarriers increasing their accumulation in the tumor and decreased their build up in healthy organs.

Adverse side effects of different DS containing paclitaxel were assessed by measuring apoptosis induction in the tumor and different organs (Fig. 5). Similar to cytotoxicity, the delivery of the anticancer drug by nanocarriers substantially enhanced their ability to induce apoptosis in the tumor but did not prevent adverse side effects of the treatment. In general, apoptosis induction in the tumor and organs correlated with organ distribution of nanocarriers. Tumor targeting dramatically improved the situation leading to an increase in the apoptosis induction in the tumor and almost complete elimination of drug adverse side effects. It should be stressed, that similar to the aforementioned results, tumor targeting also decreased the variations in cell death induction between different DS (compare bar 1 for LHRH–PEG–TAX, LHRH–PAMAM–TAX and LHRH–Lip–TAX in Fig. 5).

3.6. Targeting to LHRH receptors enhances antitumor activity of anticancer delivery systems

Antitumor activity of free TAX and different non-targeted and tumor-targeted DS were compared in experiments on nude mice bearing xenografts of A549 human lung cancer cells. It was found that even non-targeted DS containing paclitaxel were significantly more effective in limiting tumor growth when compared with free drug (Fig. 6). We also found differences between various non-targeted DS: dendrimeric DS was the least effective, while PEG polymer-based DS was the most effective in terms of the suppression of tumor growth (compare curves 6 in Fig. 6a–c). The average tumor size at the end of the treatment was 839±25, 684±37 and 625±16 mm^3 for non-targeted dendrimeric, liposomal, and polymeric

DS respectively (Means±SD, $P<0.05$ between all series). Targeting of cancer cells by LHRH peptide significantly enhanced antitumor activity of all systems and leveled down the differences between various nanocarriers. Finally, all tumor-targeted DS containing paclitaxel caused significant and comparable tumor shrinkage. The average tumor size at the end of the treatment was 4.03±0.21, 4.07±0.39 and 3.93±0.29 folds smaller for targeted dendrimeric, liposomal, and polymeric DS respectively when compared with non-targeted systems (Means±SD, $P> 0.05$ between all series).

4. Discussion

In the present study, we characterized and compared in similar experimental conditions three different types of non-targeted and tumor-targeted delivery systems carrying a similar payload. We selected DS with linear PEG polymer, star-like PAMAM dendrimer, and liposomal carriers. The selection of such systems was based on the following considerations. First, these nanocarriers represent the main classes of modern types of nanocarriers which are being used for cancer imaging and chemotherapy [34–36]. Second, these delivery systems employ three of the most widely used types of nanocarrier architecture: linear polymers, branched polymers, and liposomes. Third, they also cover almost the entire range of the most frequently exploited nanocarrier sizes (5–150 nm). Four, the same anticancer drug delivered by such different nanocarriers possesses substantially different properties including cellular internalization, cytotoxicity, tumor and body distribution, adverse side effects on healthy organs, and antitumor activity.

Each of these nanocarriers was targeted specifically to the tumor by adding a targeting moiety — a synthetic analog of luteinizing hormone-releasing hormone. LHRH peptide is a ligand for the receptors that are overexpressed in plasma membrane of breast, ovarian, and prostate cancer cells [26,29,37] and, as found in the present study, in some types of lung cancer cells. In contrast, the expression of these receptors in healthy organs in most cases is non-detectable [23,38]. It should be stressed, that, in contrast to the therapeutic applications of LHRH hormone, we do not use LHRH peptide as a drug to directly treat hormone-dependent breast, ovarian cancer, and gynecological malignancies [39,40]. Instead, we are using the analog of this peptide as a targeting moiety to extracellular LHRH receptors for the direct targeting of cancer cells in concentrations which do not induce therapeutic or cytotoxic effects.

The present study was focused on the following objectives. First, by employing the tumor-specific targeting moiety, we expected to improve body distribution of different non-targeted nanocarrier-based delivery systems and increase the sensitivity and specificity of imaging and/or treatment of cancer and limit adverse side effects of the treatment on healthy organs. Second, we anticipated that targeting nanocarriers to cancer cells would enhance cellular internalization and distribution, cytotoxicity, and antitumor activity of an encapsulated anticancer drug. Third, we hypothesized that tumor targeting will be the most valuable for the least efficient types of nanocarriers, therefore diminishing the differences between DS of various architecture, size and molecular mass in terms of anticancer efficacy and adverse side effects of the treatment on healthy tissues.

We found that targeting of DS to extracellular LHRH receptors overexpressed in the plasma membrane of many types of cancer cells substantially improved internalization and intracellular distribution of the entire DS and incorporated imaging agent. Targeting also enhanced overall accumulation of a nanocarrier by cancer cells and increased the fraction of the applied dose which actually penetrates cancer cells and therefore has the potential to effectively kill the cells or increase the sensitivity of their detection by a fluorescent or other labeling. Enhanced accumulation by cancer cells of tumor-targeted DS containing an

anticancer agent led to the substantial increase in the cytotoxicity of the drug and formed the basis for its high anticancer efficacy. Moreover, high antitumor efficacy of tumor-targeted anticancer DS was accompanied by preferential accumulation of such DS specifically in tumor cells which provided low adverse side effects of cytotoxic DS on healthy organs and increased the specificity and sensitivity of cancer detection by fluorescent or other imaging agents. It is also very important that tumor-specific targeting minimized the differences between nanocarriers of distinct types of architecture, size, mass, and composition.

The results of the present study exceeded our expectations. Experimental data demonstrated that targeting to cancer cells by LHRH peptide enhanced antitumor activity of all tested DS to the exceptionally high level comparable for all types of nanocarriers. Simultaneously, targeting to tumor-specific receptors prevented serious adverse side effects of the treatment on healthy organs. Consequently, our data showed that the internalization and intracellular distribution of DS, but not size, molecular mass, composition or architecture of the carrier, play a critical role in anticancer effect of tumor-targeted chemotherapy. This conclusion could have a broad impact on the cancer drug delivery and imaging. In particular, it means that tumor-specific receptor-targeting of nanocarriers could provide for a high antitumor therapeutic activity and imaging efficacy with low adverse side effects on healthy organs for practically any type of anticancer/imaging DS. At the same time, other parameters of nanocarriers, including size, composition, architecture, etc. can be selected based on other considerations, such as type of imaging or therapeutic agents, their aqueous solubility, electric charge, chemical structure, etc. This conclusion is made for the first time in the present study and has the theoretical and practical potential for drug delivery in general and for nanoparticle cancer imaging and chemotherapy, in particular.

Acknowledgments

This work was supported in part by CA100098 and CA111766 grants from the National Cancer Institute and a LCD-23812-N grant from the American Lung Association.

References

[1]. Allen TM, Cullis PR. Drug delivery systems: entering the mainstream. Science. 2004; 303(5665): 1818–1822. [PubMed: 15031496]

[2]. Arayne MS, Sultana N. Review: nanoparticles in drug delivery for the treatment of cancer. Pak. J. Pharm. Sci. 2006; 19(3):258–268. [PubMed: 16935836]

[3]. Duncan R. The dawning era of polymer therapeutics. Nat. Rev., Drug Discov. 2003; 2(5):347–360. [PubMed: 12750738]

[4]. Duncan R. Polymer conjugates as anticancer nanomedicines. Nat. Rev., Cancer. 2006; 6(9):688–701. [PubMed: 16900224]

[5]. Gao X, Chung LW, Nie S. Quantum dots for in vivo molecular and cellular imaging. Methods Mol. Biol. 2007; 374:135–146. [PubMed: 17237536]

[6]. Grodzinski P, Silver M, Molnar LK. Nanotechnology for cancer diagnostics: promises and challenges. Expert Rev. Mol. Diagn. 2006; 6(3):307–318. [PubMed: 16706735]

[7]. Khandare JJ, Jayant S, Singh A, Chandna P, Wang Y, Vorsa N, Minko T. Dendrimer versus linear conjugate: influence of polymeric architecture on the delivery and anticancer effect of Paclitaxel. Bioconjug. Chem. 2006; 17(6):1464–1472. [PubMed: 17105225]

[8]. Malik N, Wiwattanapatapee R, Klopsch R, Lorenz K, Frey H, Weener JW, Meijer EW, Paulus W, Duncan R. Dendrimers: relationship between structure and biocompatibility in vitro, and preliminary studies on the biodistribution of 125I-labelled polyamidoamine dendrimers in vivo. J. Control. Release. 2000; 65(1–2):133–148. [PubMed: 10699277]

[9]. Majoros IJ, Myc A, Thomas T, Mehta CB, Baker JR Jr. PAMAM dendrimer-based multifunctional conjugate for cancer therapy: synthesis, characterization, and functionality. Biomacromolecules. 2006; 7(2):572–579. [PubMed: 16471932]

[10]. Mitra A, Nan A, Line BR, Ghandehari H. Nanocarriers for nuclear imaging and radiotherapy of cancer. Curr. Pharm. Des. 2006; 12(36):4729–4749. [PubMed: 17168775]

[11]. Myc A, Majoros IJ, Thomas TP, Baker JR Jr. Dendrimer-based targeted delivery of an apoptotic sensor in cancer cells. Biomacromolecules. 2007; 8(1):13–18. [PubMed: 17206782]

[12]. Patri AK, Majoros IJ, Baker JR. Dendritic polymer macromolecular carriers for drug delivery. Curr. Opin. Chem. Biol. 2002; 6(4):466–471. [PubMed: 12133722]

[13]. Popescu MA, Toms SA. In vivo optical imaging using quantum dots for the management of brain tumors. Expert Rev. Mol. Diagn. 2006; 6(6):879–890. [PubMed: 17140375]

[14]. Portney NG, Ozkan M. Nano-oncology: drug delivery, imaging, and sensing. Anal. Bioanal. Chem. 2006; 384(3):620–630. [PubMed: 16440195]

[15]. Sinha R, Kim GJ, Nie S, Shin DM. Nanotechnology in cancer therapeutics: bioconjugated nanoparticles for drug delivery. Mol. Cancer Ther. 2006; 5(8):1909–1917. [PubMed: 16928810]

[16]. Tomalia DA, Reyna LA, Svenson S. Dendrimers as multi-purpose nanodevices for oncology drug delivery and diagnostic imaging. Biochem. Soc. Trans. 2007; 35(Pt 1):61–67. [PubMed: 17233602]

[17]. Torchilin VP. Multifunctional nanocarriers. Adv. Drug Deliv. Rev. 2006; 58(14):1532–1555. [PubMed: 17092599]

[18]. Torchilin VP. Micellar nanocarriers: pharmaceutical perspectives. Pharm. Res. 2007; 24(1):1–16. [PubMed: 17109211]

[19]. True LD, Gao X. Quantum dots for molecular pathology: their time has arrived. J. Mol. Diagnostics. 2007; 9(1):7–11.

[20]. van Vlerken LE, Amiji MM. Multi-functional polymeric nanoparticles for tumour-targeted drug delivery. Expert Opin. Drug Deliv. 2006; 3(2):205–216. [PubMed: 16506948]

[21]. Wang D, Kopeckova JP, Minko T, Nanayakkara V, Kopecek J. Synthesis of starlike *N*-(2-hydroxypropyl)methacrylamide copolymers: potential drug carriers. Biomacromolecules. 2000; 1(3):313–319. [PubMed: 11710118]

[22]. Minko, T.; Khandare, JJ.; Vetcher, AA.; Soldatenkov, VA.; Garbuzenko, OB.; Saad, M.; Pozharov, VP. Multifunctional Pharmaceutical Nanocarriers, Series: Fundamental Biomedical Technologies. Torchilin, VP., editor. Vol. vol. 4. Springer; 2008. p. 309-335.

[23]. Dharap SS, Wang Y, Chandna P, Khandare JJ, Qiu B, Gunaseelan S, Sinko PJ, Stein S, Farmanfarmaian A, Minko T. Tumor-specific targeting of an anticancer drug delivery system by LHRH peptide. Proc. Natl. Acad. Sci. U. S. A. 2005; 102(36):12962–12967. [PubMed: 16123131]

[24]. Khandare JJ, Chandna P, Wang Y, Pozharov VP, Minko T. Novel polymeric prodrug with multivalent components for cancer therapy. J. Pharmacol. Exp. Ther. 2006; 317(3):929–937. [PubMed: 16469865]

[25]. Ahmed F, Pakunlu RI, Brannan A, Bates F, Minko T, Discher DE. Biodegradable polymersomes loaded with both paclitaxel and doxorubicin permeate and shrink tumors, inducing apoptosis in proportion to accumulated drug. J. Control. Release. 2006; 116(2):150–158. [PubMed: 16942814]

[26]. Dharap SS, Qiu B, Williams GC, Sinko P, Stein S, Minko T. Molecular targeting of drug delivery systems to ovarian cancer by BH3 and LHRH peptides. J. Control. Release. 2003; 91(1–2):61–73. [PubMed: 12932638]

[27]. Pakunlu RI, Wang Y, Saad M, Khandare JJ, Starovoytov V, Minko T. In vitro and in vivo intracellular liposomal delivery of antisense oligonucleotides and anticancer drug. J. Control. Release. 2006; 114:153–162. [PubMed: 16889867]

[28]. Wang Y, Minko T. A novel cancer therapy: combined liposomal hypoxia inducible factor 1 alpha antisense oligonucleotides and an anticancer drug. Biochem. Pharmacol. 2004; 68(10):2031–2042. [PubMed: 15476674]

[29]. Dharap SS, Minko T. Targeted proapoptotic LHRH-BH3 peptide. Pharm. Res. 2003; 20(6):889–896. [PubMed: 12817893]

[30]. Minko T, Kopeckova P, Kopecek J. Chronic exposure to HPMA copolymer-bound adriamycin does not induce multidrug resistance in a human ovarian carcinoma cell line. J. Control. Release. 1999; 59(2):133–148. [PubMed: 10332049]

[31]. Minko T, Kopeckova P, Pozharov V, Kopecek J. HPMA copolymer bound adriamycin overcomes MDR1 gene encoded resistance in a human ovarian carcinoma cell line. J. Control. Release. 1998; 54(2):223–233. [PubMed: 9724909]

[32]. Ahmed F, Pakunlu RI, Srinivas G, Brannan A, Bates F, Klein ML, Minko T, Discher DE. Shrinkage of a rapidly growing tumor by drug-loaded polymersomes: pH-triggered release through copolymer degradation. Mol. Pharmacol. 2006; 3(3):340–350.

[33]. Geng Y, Dalhaimer P, Cai S, Tsai R, Tewari M, Minko T, Discher D. Soft filaments circulate longer than spherical particles — shape effects in flow and drug delivery. Nature Nanotech. 2007; 2:249–255.

[34]. Khandare J, Minko T. Polymer–drug conjugates: progress in polymeric prodrugs. Progr. Polym. Sci. 2006; 31:359–397.

[35]. Khandare JJ, Minko T. Polymer–drug conjugates: progress in polymeric prodrugs. Progr. Polym. Sci. 2006; 31:359–397.

[36]. Minko, T.; Khandare, J.; Jayant, S. Macromolecular Engineering: From Precise Macromolecular Synthesis to Macroscopic Material Properties and Application. Matyjaszewski, K.; Gnanou, Y.; Leibler, L., editors. Vol. vol. 4th. Wiley-VCH Verlag GmbH & Co.; Weinheim: 2007. p. 2541-2595.

[37]. Minko T, Dharap SS, Pakunlu RI, Wang Y. Molecular targeting of drug delivery systems to cancer. Curr. Drug Targets. 2004; 5(4):389–406. [PubMed: 15134222]

[38]. Chandna P, Saad M, Wang Y, Ber E, Khandare J, Vetcher AA, Soldatenkov VA, Minko T. Targeted proapoptotic anticancer drug delivery system. Mol. Pharmacol. 2007; 4(5):668–678.

[39]. Burger CW, Prinssen HM, Kenemans P. LHRH agonist treatment of breast cancer and gynecological malignancies: a review. Eur. J. Obstet. Gynecol. Reprod. Biol. 1996; 67(1):27–33. [PubMed: 8789746]

[40]. Sharma R, Beith J, Hamilton A. Systematic review of LHRH agonists for the adjuvant treatment of early breast cancer. Breast. 2005; 14(3):181–191. [PubMed: 15927827]

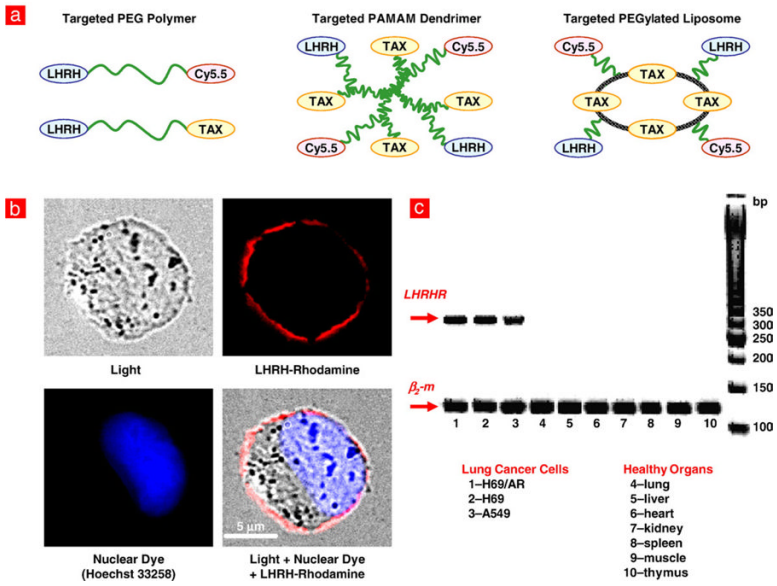

Fig. 1.

Tumor-specific receptor-targeted delivery systems for cancer imaging and treatment. a, Three different types of tumor-targeted delivery systems (linear PEG polymer, branched PAMAM dendrimer and PEGylated liposomes). A synthetic analog of LHRH decapeptide, near-infrared cyanine dye Cy5.5 and paclitaxel (TAX) were used as a tumor targeting moiety, imaging agent, and anticancer drug respectively. b–c, Luteinizing hormone-releasing hormone (LHRH) receptors are overexpressed in the plasma membrane of cancer cells and are not expressed detectably in normal visceral organs. b, Human non-small A549 lung carcinoma cells were incubated with LHRH peptide labeled with Rhodamine(red fluorescence). Nuclei of the cells were labeled with Hoechst 33258 dye (blue fluorescence). Labeled LHRH peptide was localized predominantly in the plasma membrane. c, The expression of LHRH receptors was measured by reverse transcription polymerase chain reaction (RT-PCR) in human drug sensitive H69 (1) and multidrug resistant H69/AR (2) small-cell lung cancer cells and A549 non-small cell lung cancer cells (3) as well as in mRNA isolated from healthy visceral organs (4 — lung, 5 — liver, 6 — heart, 7 — kidney, 8 — spleen, 9 — muscle, 10 — thymus).

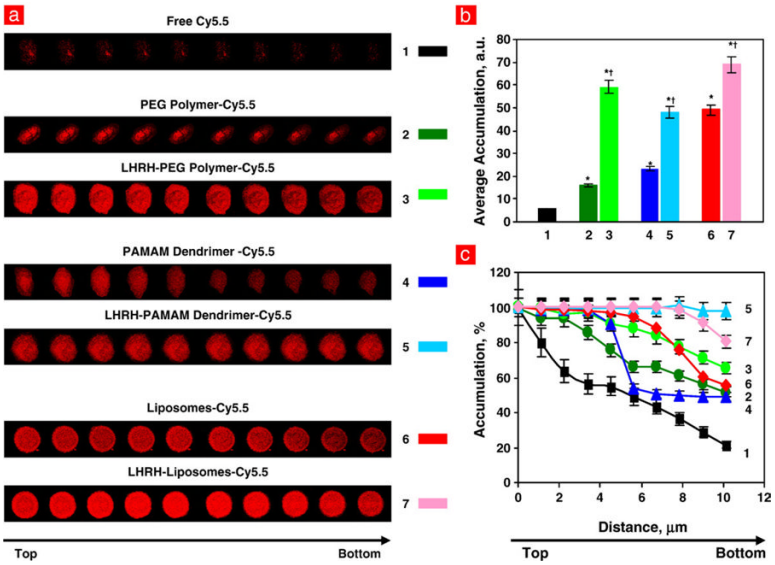

Fig. 2.

LHRH peptide as a tumor targeting moiety enhances penetration and normalizes intracellular distribution of different nanocarriers in cancer cells. a, Confocal microscopy fluorescent images of human A549 lung carcinoma cells incubated for 24 h with free near-infrared dye Cy5.5 (red fluorescence), non-targeted and cancer-targeted different delivery systems labeled with Cy5.5 (*z*-series from the top to the bottom). b, c, Quantitative analysis of the accumulation and distribution inside the cells of labeled delivery systems.

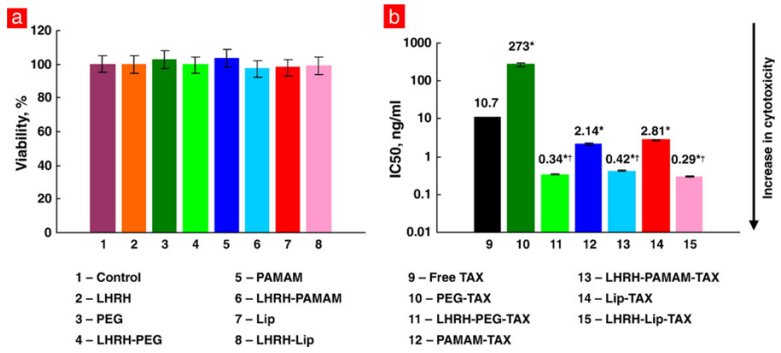

Fig. 3.

LHRH peptide significantly increases the cytotoxicity of paclitaxel incorporated into different nanoscale-based delivery systems. a, Components of delivery systems are not toxic for human A549 lung carcinoma cells. b, IC_{50} doses for free paclitaxel (TAX), non-targeted and cancer cell-targeted delivery systems. Means ± SD are shown. $*P < 0.05$ when compared with free paclitaxel. $^{\dagger}P < 0.05$ when compared with corresponding non-targeted system.

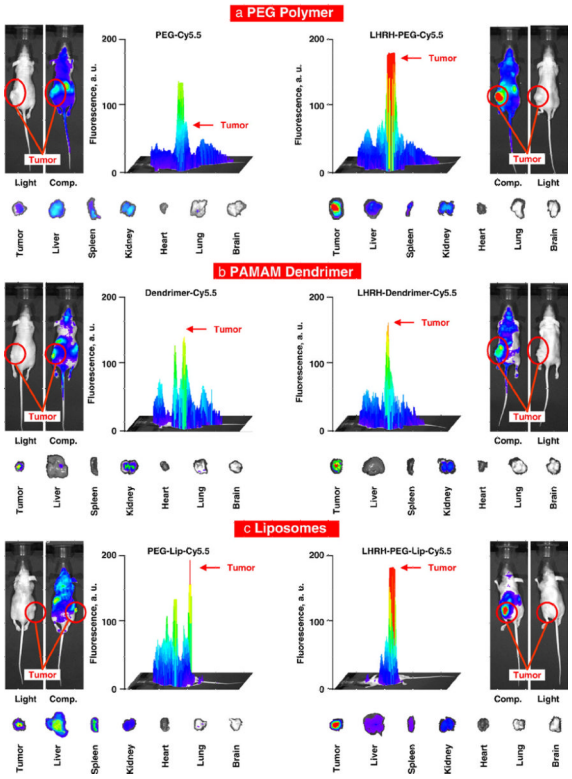

Fig. 4.

LHRH peptide as a tumor-specific targeting moiety increases accumulation of different delivery systems in the tumor of mice bearing xenografts of human A549 lung carcinoma and limits their buildup in healthy organs. The nanocarriers were labeled with near-infrared dye Cy5.5, injected intravenously into the mice. The distribution of labeled nanocarriers was analyzed in live anesthetized animals 48 h after injection using IVIS Xenogen imaging system. The intensity of fluorescence is expressed by different colors with blue color reflecting the lowest intensity and red is indicative of the highest intensity. After measuring the distribution of fluorescence in the entire animal, tumor and healthy organs were excised and their fluorescence were registered and processed by the imaging system. Representative images are shown.

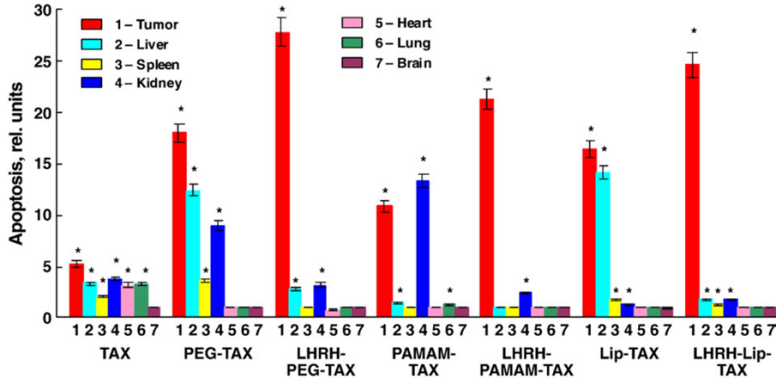

Fig. 5.

Targeting by LHRH peptide enhances apoptosis induction in the tumor and prevents adverse side effects on healthy organs of different delivery systems containing paclitaxel. Mice bearing xenografts of human A549 lung carcinoma were treated with free paclitaxel and different delivery systems with the same dose of TAX (2.5 mg/kg). The enrichment of histone-associated DNA fragments (mono- and oligonucleosomes) per gram tissue in the tumor and organs of control animals was set to unit 1, and the degree of apoptosis was expressed in relative units. Means ± SD are shown. *P <0.05 when compared with control (animals treated with saline).

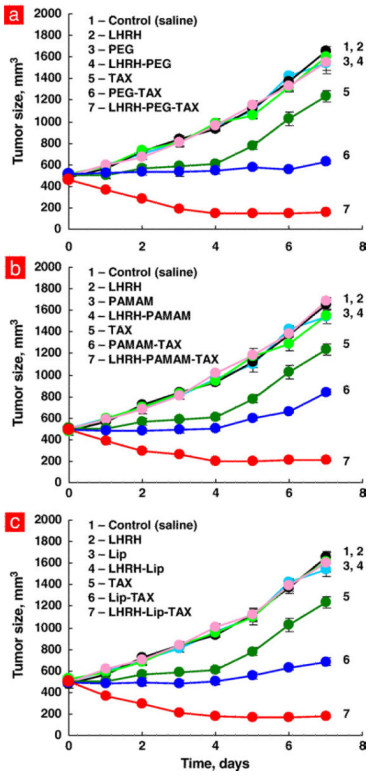

Fig. 6.

Tumor targeting by LHRH peptide enhances antitumor activity of paclitaxel delivered by different nanocarriers. Mice bearing xenografts of human A549 lung carcinoma were treated with free paclitaxel and different delivery systems with the same dose of TAX (2.5 mg/kg). Tumor volume was measured by a caliper every day for 7 days after the treatment. Means ± SD are shown.